J Mater Sci (2006) 41:6403–6408
DOI 10.1007/s10853-006-0732-1

An investigation of the effect of Ti, Pd and Zr on the dehydriding kinetics of MgH_2

**L. E. A. Berlouis · P. Honnor · P. J. Hall ·
S. Morris · S. B. Dodd**

Received: 17 June 2004 / Accepted: 13 July 2005 / Published online: 22 August 2006

Abstract The effect of additives Ti, Pd and Zr on the rate of hydrogen desorption from MgH_2 is investigated using high-pressure differential scanning calorimetry. Van't Hoff analysis as well as X-ray powder diffraction measurements confirm that no new intermetallic phases are formed in these systems but enhanced dehydriding kinetics are obtained in the presence of Pd and Zr. For the Mg–Zr composite, Zr precipitates are formed throughout the material on heating to 500 °C but these do not grow with further thermal cycling. The desorption rate for all the composites was found to increase with temperature as well as pressure difference between experimental and equilibrium pressures. A value of 114 ± 4 kJ mol^{-1} was obtained for the activation energy for dehydriding of the Mg–Ti–Pd composite.

Introduction

Despite having a very high hydrogen capacity of 7.6 wt%, MgH_2 suffers from poor dehydriding kinetics, a high hydride stability and very poor cycling stability. The drive to develop more suitable Mg-composite materials and hence overcome some of these limitations has been extensive through the use of metals [1, 2], non-metals [1, 3] and intermetallics [4–9]. Depending on the method of preparation of these composite materials, an enhancement in both the thermodynamic properties and kinetics, with respect to pure Mg, have been reported and these have been associated with specific physical processes that occur during the preparation. For example, during the mechanical alloying of Mg with Ni, a new intermetallic phase (Mg_2Ni) with a correspondingly lower plateau temperature but also lower hydride content (3.6 wt%) can result. Furthermore, the presence of Ni acts as a strong catalyst for the dissociation of hydrogen.

In this work, the mechanical alloying (ball-milling) [1] technique, as well as physical vapour deposition (PVD) [10], were employed in the preparation of the Mg composites studied. The additives used were Ti, Pd and Zr. Some of the resulting composites have already been investigated [1, 8] and favourable kinetics have been reported. Several steps are involved in the hydriding and dehydriding of Mg, viz., surface dissociation of hydrogen followed by diffusion of Mg interstitials in the hydriding step and nucleation of the Mg phase and movement of the phase boundary in the dehydriding step [11]. The latter can be further expanded [12] into a phase transformation from hydride into an α-solid solution and hydrogen atoms; the flow of the hydrogen through the growing solid solution phase by Knudsen flow or ordinary gaseous diffusion; the change of the hydrogen from the absorbed state into a surface adsorbed state and finally, the associative

---

L. E. A. Berlouis (✉) · P. Honnor
Pure and Applied Chemistry, University of Strathclyde,
Glasgow G1 1XL, UK
e-mail: l.berlouis@strath.ac.uk

P. J. Hall
Chemical and Process Engineering, University
of Strathclyde, Glasgow G1 1XJ, UK

S. Morris · S. B. Dodd
Structures and Materials Centre-A7, QinetiQ Ltd., Cody
Technology Park, Farnborough, Hants GU14 0LX, UK

chemisorption and surface diffusion of the hydrogen atoms. The experimental conditions determine which process becomes the rate determining step. In this work, we concentrated on investigating the dehydriding step using the technique of high pressure differential scanning calorimetry (HP-DSC). The experiments, carried out under isothermal as well as isobaric conditions for constant loadings should enable us to delineate between some of the various steps involved in the dehydriding kinetics of the system. A comparison of our data on the Mg composites to that data obtained by Bohmhammel et al. [13] would also be helpful in the analysis.

Experimental

The Mg + 10 wt% Ti and Mg + 10 wt% (Pd and Ti) samples were prepared by the mechanical alloying process [14]. Essentially, a high energy milling system (Aerospace Metal Composites) utilising a steel mill bowl was operated within an inert gas atmosphere. Powder loading into the mill was of the order of 1 kg and process times were limited by agglomeration of the milled powder and varied for each alloy combination but was typically 100 min. Oxygen content was maintained at ppm levels during processing and a process control agent (PCA) (stearic acid) was added at 0.5 wt% to limit agglomeration of the particles. For the Mg–Zr composite, the method of preparation was PVD. Here, the composites were obtained by co-evaporating magnesium from a boiler with Zr evaporated by electron beam from a rod feed. The composition of the vapour deposit was controlled by varying the temperature of the magnesium boiler. The evaporation rate of the Zr was maintained at a constant rate. The deposits were collected on an aluminium plate 200 × 200 mm and thicknesses up to 2 mm were produced. Figure 1 shows an SEM of the fracture surface of a PVD Mg–Zr deposit. It can be seen from the figure that column-like deposits [15] are formed, with the growth perpendicular to the deposit surface. As can be seen the column widths are in the region of 0.5–1.0 µm diameter. The spacing between the columns provides adequate initial pathways for hydrogen movement through the thickness of the deposit, which then undergoes further fracturing on subsequent hydriding/dehydriding cycles.

The HP-DSC employed was a Mettler-Toledo DSC HP27 controlled by a TC11 processor and interfaced to a personal computer. The experimental set-up has been described elsewhere [16]. Essentially, temperature scanning (30–550 °C) at 31.5 bar H_2 pressure was carried out, with the enthalpy of dehydriding and rehydriding recorded during the heating and cooling stages, respectively. The isothermal dehydriding experiments were only initiated once constant values of the enthalpies were obtained during temperature cycling. Once these criteria had been met, isothermal dehydriding was carried out by reducing the pressure in the HP-DSC from 31.5 to 3.5 bar at the set temperature. The decomposition of the metal hydride formed during cooling to that temperature thus occurred spontaneously on pressure reduction and the heat flow corresponding to the hydrogen desorption was recorded by the HP-DSC. Dehydriding at constant temperature as a function of dehydriding pressure was achieved by allowing the fully formed hydride to cool to the set temperature and then reducing the pressure to different values below the equilibrium pressure for that temperature.

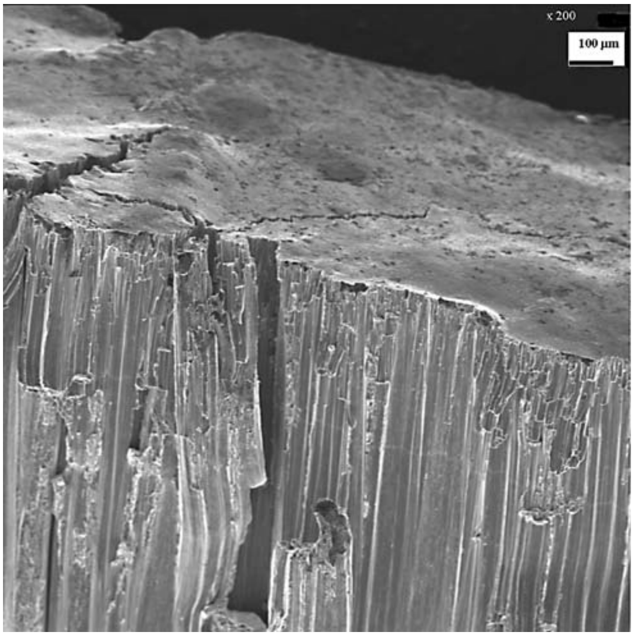

Fig. 1 SEM picture of PVD layer of magnesium–zirconium composite layer

Results and discussion

Optical microscopy examination on the MA powders indicated that the alloy additions were not held in solid solution. Small particles, typically 10 µm in size, of alloy addition were uniformly distributed within the matrix and the highly worked structure generated by the MA was found to be sub-micron in nature. Bulk chemical analysis on the powders indicated that Fe

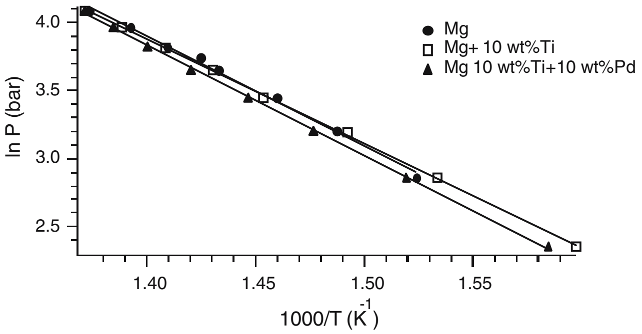

Fig. 2 Van't Hoff plots, derived from the HP-DSC data, for various Mg composites

pick up during processing was negligible with less than 0.1 wt% for the longest milling times. Oxygen levels cannot be determined for magnesium from bulk chemical analysis but X-ray powder diffraction (XRD) indicated that with additions of stearic acid there was evidence of MgO and β-MgH$_2$ but no Mg$_4$C. Van't Hoff analysis (Fig. 2) was carried out on the Mg composites using the peak temperature values for the desorption process from the HP-DSC. The data evaluated for the enthalpy ($\Delta H \sim -70$ kJ mol^{-1}) and entropy ($\Delta S \sim -130$ J mol^{-1} K^{-1}) are in broad agreement with those reported in the literature [17] for pure Mg and suggest that no additional hydride phases had formed either during the production stage or during hydrogenation. In addition, detailed analysis on the material produced prior to hydrogen storage studies demonstrated that the magnesium does not form intermetallics with Ti, Pd or Zr additions [10, 14]. XRD analysis carried out on two of the samples is shown in Fig. 3. Peaks, albeit small in intensity relative to the Mg ones, are found at 2θ angles of 38.4° and 40.1° for the Mg + Ti composite (Fig. 3a) and at 40.1° for the Mg–Ti–Pd composite (Fig. 3b). These are attributable to Ti and Pd, respectively. XRD analysis did not reveal any additional peaks or shift in the 2θ values from those of the constituent elements.

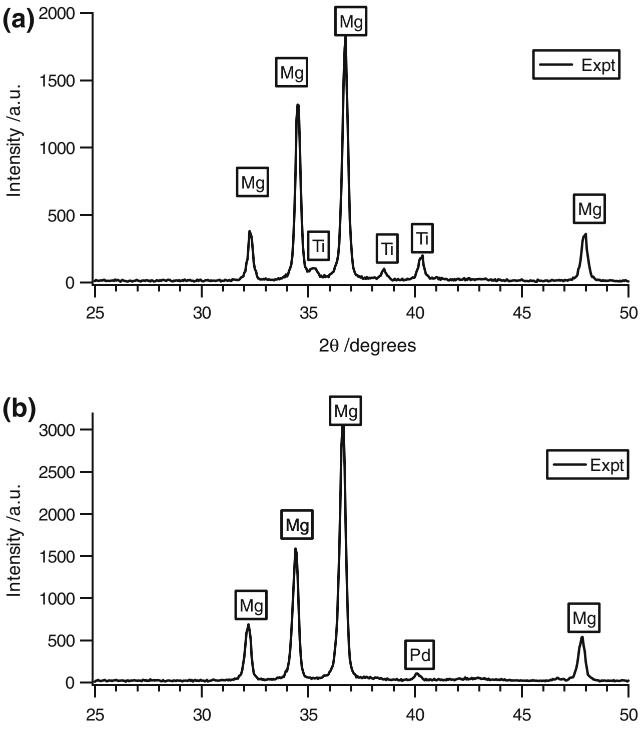

Fig. 3 X-ray powder diffraction of (**a**) Mg + 10 wt% Ti and (**b**) Mg + 10 wt% Ti + 10 wt% Pd composites

The presence of the non-Mg components in the composite would then serve only to improve the kinetics of the hydriding/dehydriding reaction, and in particular, the stage involving the dissociation/association of the hydrogen on the composite surface. This could occur by disrupting the oxide at the surface of the composite, actively catalysing the dissociation of hydrogen or simply pinning the nanoscale microstructure and inhibiting grain growth. The HP-DSC curve for the hydriding reaction of the Mg (10 wt% Ti + P-CA) sample under 31.5 bar H$_2$ and its subsequent dehydriding at 390 °C as the pressure was reduced to 3.5 bar is shown in Fig. 4. This data is very similar to that reported by Bohmhammel et al. [13] for the absorption and desorption in MgH$_2$. However, no clear differentiation of the three-step sequence of the reaction (as noted by Bohmhammel et al. [13]) could be made from the data of Fig. 4. In our experiments, the hydriding exotherm had a very sharp onset which varied insignificantly (409 ± 1 °C) with repeated cycling.

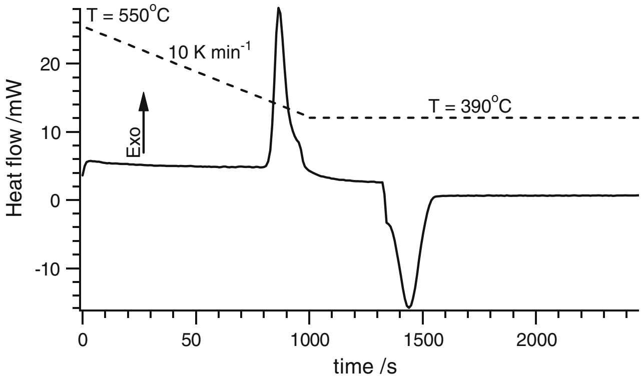

Fig. 4 HP-DSC curve for Mg composite (Mg + 10 wt% Ti). Dehydriding occurs at ~1300 s as a result of a pressure drop from 31.5 to 3.5 bar at T = 390 °C

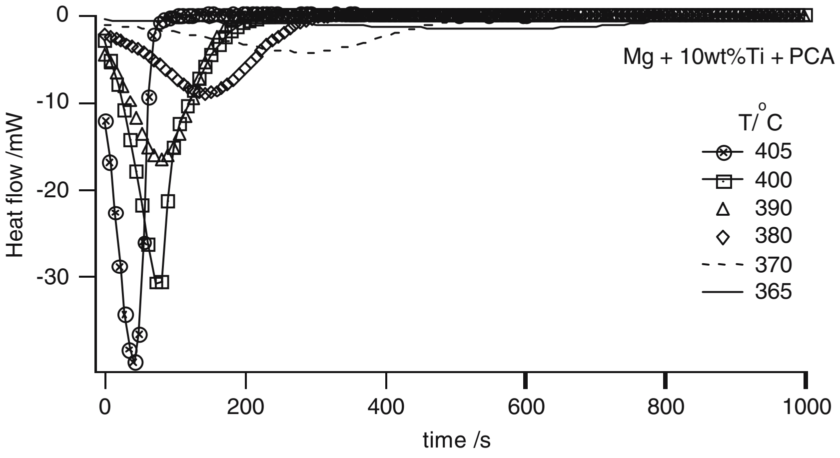

Fig. 5 Heat flow curves from HP-DSC for the dehydriding of Mg composite (Mg + 10 wt% Ti) as a function of temperature. Pressure drop from 31.5 to 3.5 bar

To examine the effect of temperature on the kinetics of the dehydriding reaction, the pressure in the HP-DSC was decreased under isothermal conditions and the results are presented in Fig. 5 for the Mg (10 wt% Ti + PCA) over the temperature range 365–405 °C. At the lower temperatures, the dehydriding rate is found

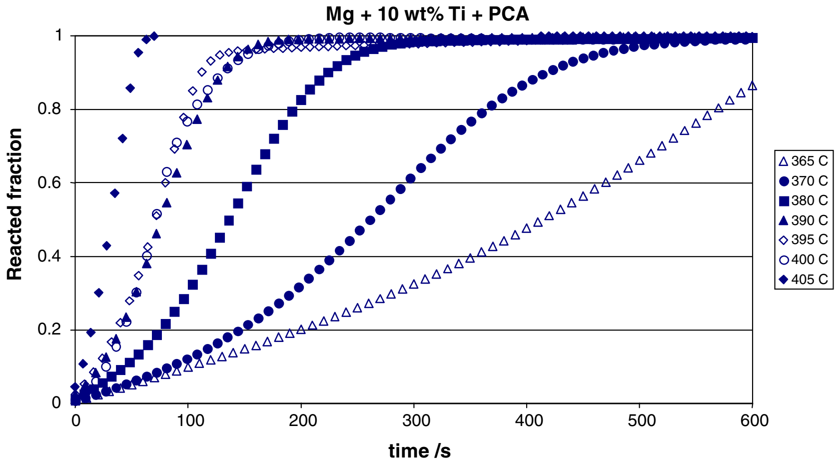

Fig. 6 Dehydriding rate of Mg composite (Mg + 10 wt% Ti) as a function of temperature. Pressure drop from 31.5 to 3.5 bar

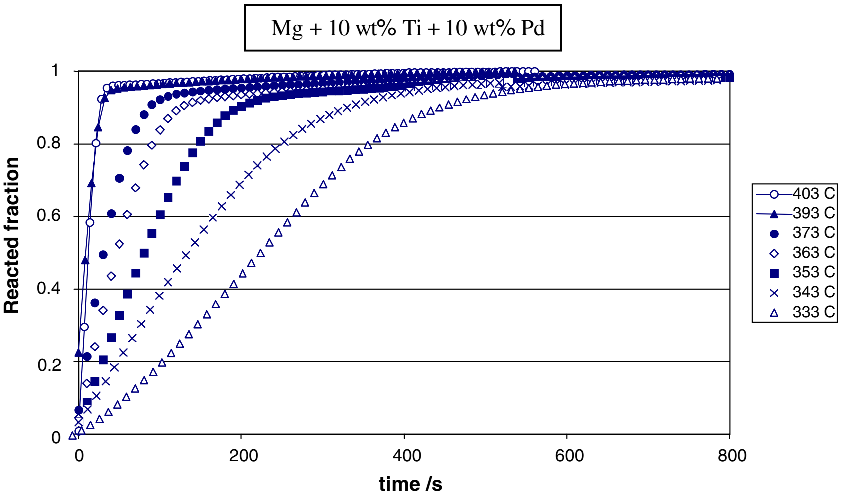

Fig. 7 Dehydriding rate of Mg composite (Mg + 10 wt% Ti + 10 wt% Pd) as a function of temperature. Pressure drop from 31.5 to 3.5 bar

Fig. 8 Dehydriding rate of Mg composite (Mg + 10 wt% Zr) at 400 °C as a function of applied pressure P_f Equilibrium pressure at 400 °C, P_e = 18.6 bar

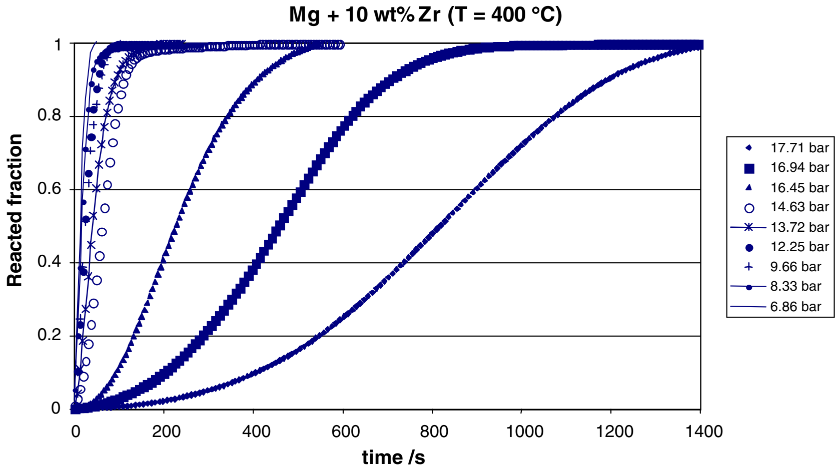

to be very slow and this is consistent with the plateau temperature of 325 °C for Mg at 3.5 bar. At the higher temperatures, rapid desorption occurred. Integration of the HP-DSC desorption curves yields the enthalpy associated with the process and so permits the calculation of the reacted fraction during dehydriding as a function of time. This is shown in Figs. 6 and 7 for the Mg composites, with Ti and with Ti + Pd, respectively. What is clear on comparison of these data is that the presence of Pd enhances the overall dehydriding reaction rate over that of Ti alone with Mg. This can be seen by examining the 363 ± 3 °C data curves where the time taken for half the hydride to decompose in the Ti composite is ~425 s whereas with the addition of the Pd, this time is reduced to ~50 s.

In our experiments, the effect of pressure on the rate can be observed from Fig. 8 which shows that the reacted fraction in the dehydriding of the Mg + 10 wt% Zr composite is reduced by a decreasing pressure difference (P_f–P_e), where P_f is the experimental pressure and P_e is the equilibrium pressure (=18.6 bar) at that temperature (400 °C). This is in essence what has been reported by Bohmhammel et al. [13] where the first order rate constant at constant temperature was found to depend linearly on the above noted pressure difference. Indeed, the data in Fig. 8 can be directly compared to that obtained by these authors [13]. In ref. 13, the time for 50% dehydriding at 9.9 bar pressure is reported as ~235 s. From Fig. 8, however, the value obtained at 9.7 bar desorption pressure is only 24 s. It is thus evident that in our data, a substantial increase in the dehydriding kinetics is found in the presence of the 10 wt% Zr. It has to be noted, however, that our desorption experiments were carried out at 400 °C whereas those of ref. 13 were at 390 °C. Nevertheless, it is apparent that both Pd and Zr play a major role in facilitating the dehydriding of the Mg hydride. Whereas Pd is well known for its dissociative action on hydrogen and so enabling the rapid diffusion of atomic hydrogen into the composite material, the action of Ti and particular Zr is, however, less clear. The contribution of Ti and Zr additions might be to pin the fine structure and prevent nucleation and growth of the Mg nanocrystals. This would maintain the high kinetics imparted by the large area of grain boundary networks, which allows for the rapid diffusion of hydrogen in the material. The enthalpies of formation for the hydrides of Ti and Zr are high and these elements are thus unlikely to participate in the hydriding. The TEM picture of Fig. 9 shows the Mg–Zr composite after heating to ~500 °C. Zr precipitates in the size range of 10–20 nm can be observed in the Mg,

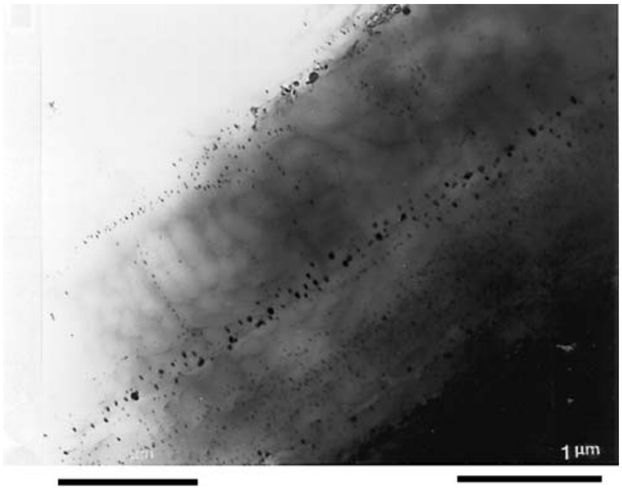

Fig. 9 TEM picture of Mg–10 wt% Zr composite after heating to 500 °C. Black spots are Zr precipitates (~10–20 nm) on the Mg surface

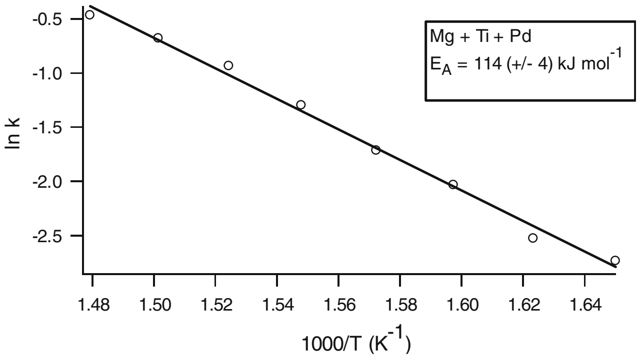

Fig. 10 Arrhenius plot for the dehydriding of the Mg–10 wt%Ti–10 wt%Pd composite

uniformly distributed throughout the microstructure. These precipitates did not grow with subsequent heating cycles. This is significant because any enhanced kinetics through the presence of the Zr on the hydrogen desorption would not be diminished with increasing cycling over the temperature range employed here.

Under isothermal conditions, the heat flow curve from the HP-DSC gives a direct measurement of the dehydriding rate of the material at that temperature. Thus, based on Stander's [11] and Song's [12] analyses for the dehydriding process, the activation energy was evaluated in the case of the Mg–Ti–Pd composite. The Arrhenius plot is shown in Fig. 10 and the value for the activation energy, E_A obtained is 114 ± 4 kJ mol^{-1}. This is unexpectedly high compared to that reported for pure Mg (ca. 100 kJ mol^{-1}) [11, 13] but it may simply reflect the different nature of the sample surfaces in the different works carried out. No surface analysis has been made at this time but we know from previous studies on the corrosion of these materials that the surface contains a network of elemental intermetallic material, which changes the nature of the oxide layers formed [18]. Work is currently underway to explore the effect of changing the additive concentration in the composite and also to quantify and explain its effect in reducing the activation energy for the process. More importantly, the data and analysis carried out will examine which of the various steps in the dehydriding process of the Mg + 10 wt% Zr composite is most influential in decreasing the activation energy.

Conclusions

High pressure differential calorimetry has been used to examine the decomposition rate of magnesium hydride in the presence of Ti, Pd and Zr additives. Although no new phases are indicated during the MA and PVD preparation of the Mg composites, enhanced kinetics for hydrogen desorption is reported in the presence of Pd and Zr additives. Zr precipitates of the order of ~10–20 nm are found in the Mg–Zr composites on heating to 500 °C. Significantly, there is no change in the size of the precipitates with repeated thermal cycles. The desorption rate was found to increase with temperature as well as pressure difference between working and equilibrium pressures. A value of 114 ± 4 kJ mol^{-1} was obtained for the activation energy for dehydriding of the Mg–Ti–Pd composite.

References

1. Zaluska A, Zaluski L, Ström-Olsen JO (1999) J Alloys Comp 288:217
2. Higuchi K, Yamamoto K, Kajioka H, Toiyama K, Honda M, Orimo S, Fujii H (2002) J Alloys Comp 330:526
3. Imamura H, Sakasai N, Kajii Y (1996) J Alloys Comp 232:218
4. Nagai H, Tomizawa H, Ogasawara T, ShojiKI (1990) J Less-Common Met 157:15
5. Orimo S, Fujii H (1998) Intermetallics 6:185
6. Orimo S, Züttel A, Ikeda K, Saruki S, Fukunaga T, Fujii H, Schlapbach L (1999) J Alloys Comp 293–295:437
7. Terxieva M, Khrussanova M, Peshev P, Radev D (1995) Int J Hydrogen Energy 20:53
8. Dutta K, Mandal P, Ramakrishna K, Srivastava ON (1994) Int J Hydrogen Energy 19:253
9. Guoxian L, Erde W, Shoushi F (1995) J Alloys Comp 223:111
10. Gardiner RW, Viney BW (1995) 'Production of bulk alloys by PVD', 124th TMS Annual meeting, Las Vegas, USA
11. Stander CM (1977) J Inorg Nucl Chem 39:221
12. Song M-Y (1990) J Less-Common Met 157:155
13. Bohmhammel K, Christ B, Wolf G (1998) Thermochim Acta 310:167
14. Dodd SB, Morris S, Ward-Close M (1999) Production of Mg–Ti by MA', 128th TMS Annual meeting, San Diego, USA
15. Yamamoto K, Higuchi K, Kajioka H, Sumida H, Orimo S, Fujii H (2002) J Alloys Comp 330:352
16. Berlouis LEA, Cabrera E, Hall-Barientos E, Hall PJ, Dodd SB, Morris S, Imam MA (2001) J Mater Res 16:45
17. Bogdanovic B, Bohmhammel K, Christ B, Reiser A, Schlichte K, Vehlen R, Wolf U (1999) J Alloys Comp 282:84
18. Dodd S et al (1998) Corrosion Reviews XVI:1